Joint Bias Estimation and Localization in Factor Graph

Feihu Zhang, Daniel Malovetz, Dhiraj Gulati, Daniel Clarke and Alois Knoll

Abstract— **This paper describes a new approach for cooperative localization by using both internal and external sensors. In contrast to the state-of-the-art methods, the proposed approach analyses the statistical properties of the systematic error during the transformation phase. A factor graph is formulated which jointly estimates both the biases and the locations. The proposed approach is evaluated by using simulated data from odometry, GPS and radar measurements. The experiment demonstrates excellent performance of the proposed approach in comparison to traditional techniques.**

I. INTRODUCTION

Interest in cooperative localization has grown exponentially in the past decade (e.g. [1], [2], [3]), as it enables a vehicle to autonomously perform better environment perception. By fusing data from disparate sources, the volume of surveillance and the reliability and precision of the state estimation process are significantly increased.

Many approaches have been employed by utilizing filtering techniques to provide an on-line estimation of the positions. Classical approaches like the Kalman filter, including the Extended Kalman Filter (EKF) [4], or Unscented Kalman Filter (UKF) [5], are considered as the workhorse to recursively calculate the posterior mean and covariance.

An alternative solution, compared to filtering techniques, is the graph-based formulations for batch processing. The benefit is the flexibility to nonlinear models in contrast to filtering techniques. It addresses the nonlinear issues by using optimization algorithms such as Gauss-Newton iterations or the Levenberg-Marquardt algorithm [6]. Many approaches have been developed like the $\sqrt{\text{SAM}}$ algorithm[7], its incremental variant iSAM [8] and the g^2o framework [9].

In practice, as the data is acquired from disparate sensors with heterogeneous capabilities, the transformations often introduce systematic errors in cooperative localization. Thus, sensor registration is considered to eliminate the systematic errors. Various approaches have been investigated and divided into centralized [10] and decentralized solutions [11], [12]. The related work has already demonstrated some preliminary results. However, the position is often overestimated without the ground-truths.

In this paper, we analyze the statistical properties of the systematic errors with respect to the mean and covariance [13], [14]. Then, the nonlinear least square method is utilized to jointly estimate biases and positions from noisy measurements.

The remainder of this paper is structured as follows: Sec. II briefly describes the background of the cooperative localization. Sec. III introduces more details of the nonlinear least square optimization. Sec. IV presents experimental results. Finally, the paper is concluded in Sec.V.

Feihu Zhang, Dhiraj Gulati are with the fortiss GmbH, München, Germany, e-mail: {zhang,gulati}@fortiss.org.

Daniel Clarke is with the The Centre for Electronic Warfare, Cranfield University, The Defence Academy of the United Kingdom, Shrivenham, Swindon, SN6 8EH, UK., e-mail: d.s.clarke@cranfield.ac.uk.

Daniel Malovetz and Alois Knoll are with the Technische Universität M"unchen, Garching bei München, Germany, e-mail: daniel.malovetz@tum.de, knoll@in.tum.de.

II. BACKGROUND DESCRIPTION

In this section, the cooperative localization is achieved by fusing data from simulated GPS, odometry and radar. We choose these sensors as they each offer a disparate way of observing the state of the vehicle (absolute location, relative change in location and location of an external target). The description of the proposed scenario is as follows:

- Using GPS, the ego-vehicle is able to localize itself in the 2D Cartesian coordinate system.
- Using odometry, the ego-vehicle is able to measure the movement in the 2D Cartesian coordinate system.
- Using radar, the ego-vehicle is able to localize itself in the 2D polar coordinate system.

Measurements from both GPS and odometry consist of the ground-truth and random noises, whereas radar measurements consist of the ground-truth, random noise and the bias.

Fig. 1 shows the measurements from both unbiased GPS and biased radar sensors in the global coordinate system. Although radar has high precision, the systematic error is significantly influenced by the bias. The goal of this paper is to take the systematic error into account as part of the state estimation process in order to jointly estimate both the sensor bias and vehicle position.

III. NONLINEAR LEAST SQUARE OPTIMIZATION

In this section, the factor graph is described to handle the nonlinear issues during the estimation.

A. Overview of factor graph

A factor graph is a bipartite graph which explains the complex functions with simpler functions. Hence it allows to compose complex problems using local computations. In general, a factor graph could be implemented in various models including Bayesian networks [15], Markov random fields [16] and junction graphs [17].

In this paper, the entire trajectory is estimated as an optimization problem by using the factorized probability distribution. The localization is then represented by estimating the trajectory $\mathbf{x} = \{x_i | i \in 0, ..., n\}$ given a set of observations from GPS $\mathbf{z}^g = \{\mathbf{z}^g | i \in 0, ..., n\}$, radar

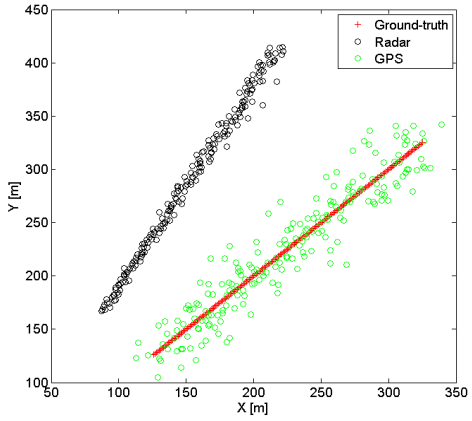

Fig. 1: Measurements from both unbiased GPS and biased radar sensors

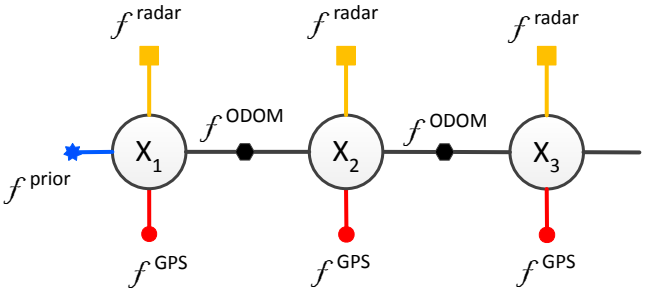

Fig. 2: Factor graph for localization

$\mathbf{z}^r = \{z^r | i \in 0, ..., n\}$ and odometry $\mathbf{u} = \{u | i \in 0, ..., n\}$. Thus the joint density is written as:

$$P(\mathbf{x}, \mathbf{z}^g, \mathbf{z}^r, \mathbf{u}) \propto P(x_0) \prod_i^n P(x_{i+1}|x_i, u_i) \prod_k^m P(z_k|x_{i_k}) \tag{1}$$

where $z_k \in \{\mathbf{z}^g, \mathbf{z}^r\}$ denotes the measurement, originating from either GPS or radar.

Fig. 2 shows a simple graphical representation of the distribution in form of a factor graph. Note that the factorization is done based on Gaussian distributions for the process and measurement models as:

$$\begin{aligned} x_i = f_i(x_{i-1}, u_i) - w_i \Leftrightarrow P(x_{i+1}|x_i, u_{i+1}) \\ \propto \exp(-\frac{1}{2}||f_i(x_{i-1}, u_i) - x_i||^2_{\Gamma_i}) \end{aligned} \tag{2}$$

$$\begin{aligned} z_k = h_k(x_{i_k}) - v_k \Leftrightarrow P(z_k|x_{i_k}) \\ \propto \exp(-\frac{1}{2}||h_k(x_{i_k}) - z_k||^2_{\Sigma_k}) \end{aligned} \tag{3}$$

where h and f denote the measurement and process models, and v and w are the corresponding noises with covariance matrices Σ_k and Γ_i.

In this paper, the goal is to calculate the maximum likelihood estimation (MLE) by using the nonlinear least square method:

$$\begin{aligned} \bar{\theta} = \text{argmax} P(\theta|\mathbf{z}, \mathbf{u}) = \\ \text{argmin}\{\sum_{i=1}^{n} ||f_i(x_{i-1}, u_i) - x_i||^2_{\Gamma_i} + \sum_{k=1}^{m} ||h_k(x_{i_k}) - z_k||^2_{\Sigma_k}\} \end{aligned} \tag{4}$$

Since radar measurements are acquired in polar coordinates, a nonlinear transformation between polar and Cartesian coordinate is established to use radar measurements.

B. Systematic error and sensor bias

This section summarizes the statistic properties of the systematic error, by using our previous work in [18]. Assuming radar also contains bias, the corresponding measurement is thus defined as:

$$r_m = \bar{r} + r_b + \tilde{r}; \tag{5}$$

$$\theta_m = \bar{\theta} + \theta_b + \tilde{\theta}; \tag{6}$$

where $\bar{r}$ and $\bar{\theta}$ denote the ground truth, and r_b and θ_b denote the corresponding biases. Also $\tilde{r}$ and $\tilde{\theta}$ are assumed to be the Gaussian noises with zero mean, and standard deviations σ_r and σ_θ. Hence new measurements are acquired as follows:

$$x_m = r_m \cos\theta_m \tag{7}$$

$$y_m = r_m \sin\theta_m \tag{8}$$

The transformed measurement can also be represented as the combination of the true value and the systematic error.

$$x_m = r_m \cos\theta_m = (\bar{r} + r_b + \tilde{r}) \cos(\bar{\theta} + \theta_b + \tilde{\theta}) = \bar{x} + \tilde{x} \tag{9}$$

$$y_m = r_m \sin\theta_m = (\bar{r} + r_b + \tilde{r}) \sin(\bar{\theta} + \theta_b + \tilde{\theta}) = \bar{y} + \tilde{y} \tag{10}$$

where $\bar{x} = \bar{r}\cos\bar{\theta}$ and $\bar{y} = \bar{r}\sin\bar{\theta}$ denote the true values and $\tilde{x}$ and $\tilde{y}$ denote the systematic errors.

Rearranging Eq. (9) and Eq. (10), the representation of the systematic errors is acquired. For clarity, only the systematic error in x direction is derived which is given as:

$$\tilde{x} = r_m \cos\theta_m - \bar{r}\cos\bar{\theta} = \bar{r}[\mathbf{A} - \cos\bar{\theta}] + r_b[\mathbf{A}] + \tilde{r}[\mathbf{A}] \tag{11}$$

and

$$\begin{aligned} \tilde{x}^2 = \bar{r}^2[\mathbf{A} - \cos\bar{\theta}]^2 + r_b^2[\mathbf{A}]^2 + \tilde{r}^2[\mathbf{A}]^2 + 2\bar{r}r_b[\mathbf{A} - \cos\bar{\theta}][\mathbf{A}] \\ + 2\bar{r}\tilde{r}[\mathbf{A} - \cos\bar{\theta}][\mathbf{A}] + 2\tilde{r}r_b[\mathbf{A}]^2 \end{aligned} \tag{12}$$

where

$$\begin{aligned} \mathbf{A} = \cos\bar{\theta}\cos\theta_b\cos\tilde{\theta} - \sin\bar{\theta}\sin\theta_b\cos\tilde{\theta} \\ - \sin\bar{\theta}\cos\theta_b\sin\tilde{\theta} - \cos\bar{\theta}\sin\theta_b\sin\tilde{\theta} \end{aligned} \tag{13}$$

Thus the expectation and covariance of the systematic error can be explicitly calculated as

$$\begin{aligned} E[\tilde{x}] = \bar{r}[\cos\bar{\theta}\cos\theta_b e^{-\sigma_\theta^2/2} - \sin\bar{\theta}\sin\theta_b e^{-\sigma_\theta^2/2} - \cos\bar{\theta}] + \\ r_b[\cos\bar{\theta}\cos\theta_b e^{-\sigma_\theta^2/2} - \sin\bar{\theta}\sin\theta_b e^{-\sigma_\theta^2/2}] \end{aligned} \tag{14}$$

and

$$E[\tilde{x}^2] = \bar{r}^2[\mathbf{B} + \cos^2\bar{\theta} - 2\cos^2\bar{\theta}\cos\theta_b e^{-\sigma_\theta^2/2} + \sin 2\bar{\theta}\sin\theta_b e^{-\sigma_\theta^2/2}] + r_b^2\mathbf{B} + \sigma_r^2\mathbf{B} + 2\bar{r}r_b[\mathbf{B} - \cos^2\bar{\theta}\cos\theta_b e^{-\sigma_\theta^2/2} + \sin 2\bar{\theta}\sin\theta_b e^{-\sigma_\theta^2/2}/2] \tag{15}$$

where $\mathbf{B}$ equals

$$\mathbf{B} = \cos^2\bar{\theta}\cos^2\theta_b(1+e^{-2\sigma_\theta^2})/2 + \sin^2\bar{\theta}\sin^2\theta_b(1+e^{-2\sigma_\theta^2})/2 + \sin^2\bar{\theta}\cos^2\theta_b(1-e^{-2\sigma_\theta^2})/2 + \cos^2\bar{\theta}\sin^2\theta_b(1-e^{-2\sigma_\theta^2})/2 - \sin 2\bar{\theta}\sin 2\theta_b e^{-2\sigma_\theta^2}/2 \tag{16}$$

Similarly, the corresponding error in y direction is calculated. However, it is observed that the calculated bias has a significant influence on the systematic error, which depends on the knowledge of the ground-truth. Hence the systematic errors are calculated on condition of the noisy measurements.

Based on the Eq. (14) and Eq. (15), the conditional first and second order moments are calculated as:

$$E[E[\tilde{x}]|r_m,\theta_m] = r_m[\cos(\theta_m-\theta_b)\cos\theta_b e^{-\sigma_\theta^2} - \sin(\theta_m-\theta_b)\sin\theta_b e^{-\sigma_\theta^2} - \cos(\theta_m-\theta_b)e^{-\sigma_\theta^2/2}] + r_b\cos(\theta_m-\theta_b)e^{-\sigma_\theta^2/2} \tag{17}$$

$$E[E[\tilde{x}^2]|r_m,\theta_m] = \mathbf{C}\times[\mathbf{M}+\mathbf{D}-2\mathbf{D}\cos\theta_b e^{-\sigma_\theta^2/2} + \mathbf{F}\sin\theta_b e^{-\sigma_\theta^2/2}] + r_b^2[\mathbf{M}] + \sigma_r^2[M] + (2r_br_m - 2r_b^2)[\mathbf{M} - \mathbf{D}\cos\theta_b e^{-\sigma_\theta^2/2} + \frac{1}{2}\mathbf{F}\sin\theta_b e^{-\sigma_\theta^2/2}] \tag{18}$$

and

$$E[E[\tilde{y}]|r_m,\theta_m] = r_m[\sin(\theta_m-\theta_b)\cos\theta_b e^{-\sigma_\theta^2} + \cos(\theta_m-\theta_b)\sin\theta_b e^{-\sigma_\theta^2} - \sin(\theta_m-\theta_b)e^{-\sigma_\theta^2/2}] + r_b\sin(\theta_m-\theta_b)e^{-\sigma_\theta^2/2} \tag{19}$$

$$E[E[\tilde{y}^2]|r_m,\theta_m] = \mathbf{C}\times[\mathbf{N}+\mathbf{E}-2\mathbf{E}\cos\theta_b e^{-\sigma_\theta^2/2} - \mathbf{F}\sin\theta_b e^{-\sigma_\theta^2/2}] + r_b^2[\mathbf{N}] + \sigma_r^2[\mathbf{N}] + (2r_br_m - 2r_b^2)[\mathbf{N} - \mathbf{E}\cos\theta_b e^{-\sigma_\theta^2/2} - \frac{1}{2}\mathbf{F}\sin\theta_b e^{-\sigma_\theta^2/2}] \tag{20}$$

where

$$\mathbf{C} = r_m^2 + r_b^2 + \sigma_r^2 - 2r_m r_b$$

$$\mathbf{D} = \cos^2(\theta_m-\theta_b)\frac{1+e^{-2\sigma_\theta^2}}{2} + \sin^2(\theta_m-\theta_b)\frac{1-e^{-2\sigma_\theta^2}}{2}$$

$$\mathbf{E} = \sin^2(\theta_m-\theta_b)\frac{1+e^{-2\sigma_\theta^2}}{2} + \cos^2(\theta_m-\theta_b)\frac{1-e^{-2\sigma_\theta^2}}{2}$$

$$\mathbf{F} = \sin 2(\theta_m-\theta_b)e^{-2\sigma_\theta^2}$$

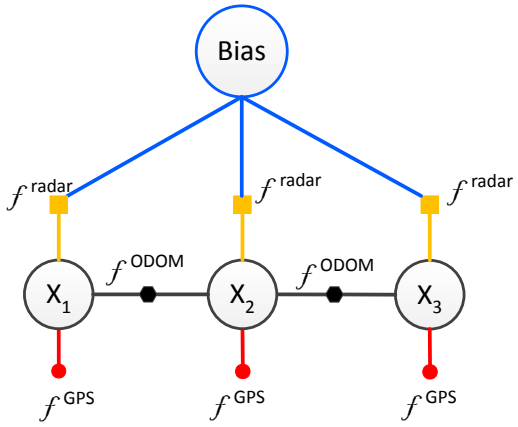

Fig. 3: Visualization of proposed factor graph

$$\mathbf{M} = \mathbf{D}\cos^2\theta_b\frac{1+e^{-2\sigma_\theta^2}}{2} + \mathbf{E}\sin^2\theta_b\frac{1+e^{-2\sigma_\theta^2}}{2} + \mathbf{E}\cos^2\theta_b\frac{1-e^{-2\sigma_\theta^2}}{2} + \mathbf{D}\sin^2\theta_b\frac{1-e^{-2\sigma_\theta^2}}{2} - \mathbf{F}\sin 2\theta_b\frac{e^{-2\sigma_\theta^2}}{2} \tag{21}$$

$$\mathbf{N} = \mathbf{E}\cos^2\theta_b\frac{1+e^{-2\sigma_\theta^2}}{2} + \mathbf{D}\sin^2\theta_b\frac{1+e^{-2\sigma_\theta^2}}{2} + \mathbf{D}\cos^2\theta_b\frac{1-e^{-2\sigma_\theta^2}}{2} + \mathbf{E}\sin^2\theta_b\frac{1-e^{-2\sigma_\theta^2}}{2} + \mathbf{F}\sin 2\theta_b\frac{e^{-2\sigma_\theta^2}}{2} \tag{22}$$

Thus the uncertainty of the transformed measurement is represented as:

$$var(\tilde{x}) = E[E[\tilde{x}^2]|r_m,\theta_m] - E^2[E[\tilde{x}]|r_m,\theta_m] \tag{23}$$

$$var(\tilde{y}) = E[E[\tilde{y}^2]|r_m,\theta_m] - E^2[E[\tilde{y}]|r_m,\theta_m] \tag{24}$$

Furthermore, to acquire an unbiased transformation, the converted measurement needs to eliminate the systematic error as follows:

$$\begin{bmatrix} r_m\cos\theta_m - E[E[\tilde{x}_n]|r_m,\theta_m] \\ r_m\sin\theta_m - E[E[\tilde{y}_n]|r_m,\theta_m] \end{bmatrix}$$

C. Graph representation

Receiving data from odometry, GPS and radar sensors, the factor graph is established with different factors and nodes. Fig. 3 illustrates the proposed factor graph with three vehicle nodes, one bias node, two odometry factors, three GPS factors and three radar factors. It is observed that the radar factors are dependent on both the measurements and the bias. Given the statistic properties of the converted measurements, the nonlinear least square method is utilized to optimize the corresponding states.

Within the factor graph presented in Fig. 3, the important contribution of this work is related to the Bias node. This node contains the unknown bias as state. The bias then is estimated and optimized by usage of the information provided by the GPS and Odometry sensors.

IV. EXPERIMENT

In this section, simulated data was used to evaluate the performance of the proposed approach both quantitatively and qualitatively. During the simulation, the GTSAM library [19] is utilized to perform the nonlinear optimization. The radar measurements have manually introduced systematic biases for both range and bearing. The odometry noise is given by zero mean, and deviation of $(0.1\text{m}, 0.1\text{m})$, the GPS noise is given by $(3\text{m}, 3\text{m})$ and the radar noise is given by $(0.1\text{m}, 0.01\text{rad})$.

To better evaluate the proposed approach, we also compare with the normal measurement implementation (original nonlinear least square method developed in GTSAM without considering the biases), and the Taylor expansion based least square method (referenced in [20]).

Fig. 4a, 4b and 4c illustrate the performance of the proposed approach in scenarios of low bias, whereas Fig. 5a, 5b and 5c exhibit the performance of the proposed approach in scenarios of high bias. It is observed that the biased measurements strongly influence the accuracy of the state estimation. However, by considering bias and eliminating the systematic error, the result of the proposed approach is close to the ground truth.

Table I and II give more details of the scenarios including the given values of biases, the estimated biases and the RMSE (root mean square error) of all approaches. To better evaluate the performance, ideal measurement RMSE (original nonlinear least square method in GTSAM with manually eliminating biases) is also given in all scenarios.

As shown in Table I, the performance between the proposed approach is close to the Taylor expansion. This is mainly due to the fact that the given biases are relatively small. Although the nonlinear issues exist, the performance of the first-order Taylor expansion is close to our approach. However, as shown in Table II, the performance of our proposed approach is significantly improved compared to the Taylor based least square method in scenarios of high biases. This is done by incorporating the proposed bias model for precisely estimating the first and second order moments. Table I and Table II demonstrate excellent performance of the proposed approach in comparison to traditional techniques.

V. CONCLUSION

In many applications where filtering and smoothing algorithms are used to fuse sensor data from disparate sources, the accuracy of the state estimation process often suffers from biased sensors. These biases can strongly influence the accuracy of the state estimation process and generally require an expensive and time consuming calibration by expert engineers.

In this paper, a graph-based solution is proposed to estimate the bias in sensor measurements by considering it as an uncertain state variable. To achieve this goal, the systematic error is analyzed with respect to its statistic properties, in reference to other sensory information. A nonlinear least square method is applied to optimize the corresponding states in the system, subsequently estimating the sensor bias. The experiment demonstrates excellent performance of the proposed approach in comparison to traditional techniques.

This work has significant benefits from the perspective of self-calibrating systems and has application across a variety of domains, in particular it has application to highly assisted and autonomous driving. In this application, it is possible for sensors to lose calibration or be physically moved over time. The introduction of this technique may allow the central fusion architecture to auto-calibrate its sensors, greatly improving the safety and reliability of the whole sensor suite.

ACKNOWLEDGMENTS

This work is partially supported by the SADA project funded by the German ministry of economics (BMWi), within the program 'IKT für Elektromobilität III'.

REFERENCES

[1] M. Baum, B. Noack, and U. D. Hanebeck, "Kalman filter-based slam with unknown data association using symmetric measurement equations," in *Multisensor Fusion and Integration for Intelligent Systems (MFI), 2015 IEEE International Conference on*, Sept 2015, pp. 49–53.

[2] G. P. Huang, A. I. Mourikis, and S. I. Roumeliotis, "A quadratic-complexity observability-constrained unscented kalman filter for slam," *IEEE Transactions on Robotics*, vol. 29, no. 5, pp. 1226–1243, Oct 2013.

[3] L. D'Alfonso, A. Griffo, P. Muraca, and P. Pugliese, "A slam algorithm for indoor mobile robot localization using an extended kalman filter and a segment based environment mapping," in *Advanced Robotics (ICAR), 2013 16th International Conference on*, Nov 2013, pp. 1–6.

[4] D. Gamage and T. Drummond, "Reduced dimensionality extended kalman filter for slam." in *BMVC*, 2013.

[5] J. Liu, H. Chen, and B. Zhang, "Square root unscented kalman filter based ceiling vision slam," in *Robotics and Biomimetics (ROBIO), 2013 IEEE International Conference on*. IEEE, 2013, pp. 1635–1640.

[6] N. Sünderhauf, "Robust optimization for simultaneous localization and mapping," 2012.

[7] F. Dellaert and M. Kaess, "Square root sam: Simultaneous localization and mapping via square root information smoothing," *The International Journal of Robotics Research*, vol. 25, no. 12, pp. 1181–1203, 2006.

[8] M. Kaess, A. Ranganathan, and F. Dellaert, "isam: Incremental smoothing and mapping," *Robotics, IEEE Transactions on*, vol. 24, no. 6, pp. 1365–1378, 2008.

[9] R. Kümmerle, G. Grisetti, H. Strasdat, K. Konolige, and W. Burgard, "g 2 o: A general framework for graph optimization," in *Robotics and Automation (ICRA), 2011 IEEE International Conference on*. IEEE, 2011, pp. 3607–3613.

[10] V. Morell-Gimenez, M. Saval-Calvo, J. Azorin-Lopez, J. Garcia-Rodriguez, M. Cazorla, S. Orts-Escolano, and A. Fuster-Guillo, "A comparative study of registration methods for rgb-d video of static scenes," *Sensors*, vol. 14, no. 5, pp. 8547–8576, 2014.

[11] X. Lin, Y. Bar-Shalom, and T. Kirubarajan, "Exact multisensor dynamic bias estimation with local tracks," *Aerospace and Electronic Systems, IEEE Transactions on*, vol. 40, no. 2, pp. 576–590, 2004.

[12] D. Huang, H. Leung, and E. Bosse, "A pseudo-measurement approach to simultaneous registration and track fusion," *IEEE Transactions on Aerospace and Electronic Systems*, vol. 48, no. 3, pp. 2315–2331, JULY 2012.

[13] S. V. Bordonaro, P. Willett, and Y. Bar-Shalom, "Unbiased tracking with converted measurements," in *2012 IEEE Radar Conference*. IEEE, 2012, pp. 0741–0745.

[14] P. Suchomski, "Explicit expressions for debiased statistics of 3d converted measurements," *IEEE Transactions on Aerospace and Electronic Systems*, vol. 35, no. 1, pp. 368–370, 1999.

[15] H.-A. Loeliger, "An introduction to factor graphs," *Signal Processing Magazine, IEEE*, vol. 21, no. 1, pp. 28–41, 2004.

[16] V. Indelman, S. Williams, M. Kaess, and F. Dellaert, "Information fusion in navigation systems via factor graph based incremental smoothing," *Robotics and Autonomous Systems*, vol. 61, no. 8, pp. 721–738, 2013.

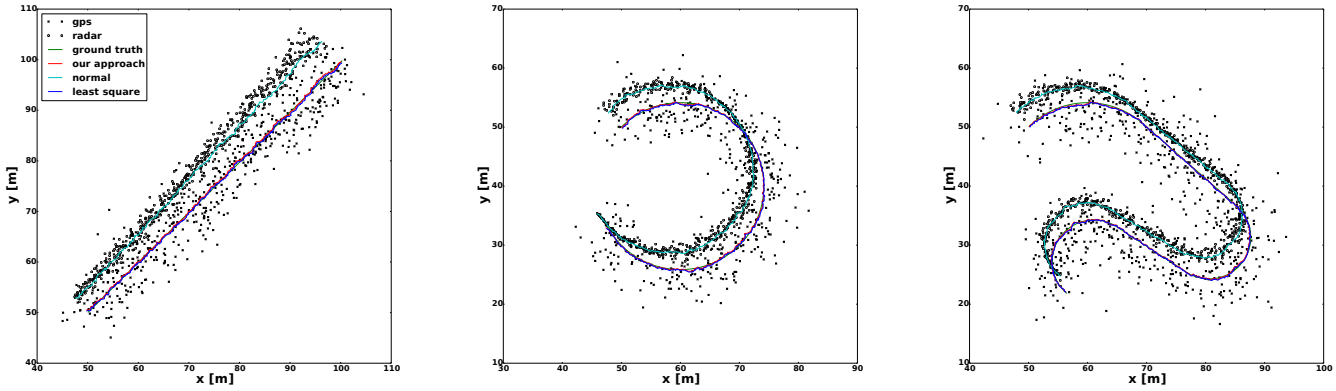

(a) Constant velocity model (b) Constant turn model (c) Complex model

Fig. 4: Performance of all approaches in low bias scenarios

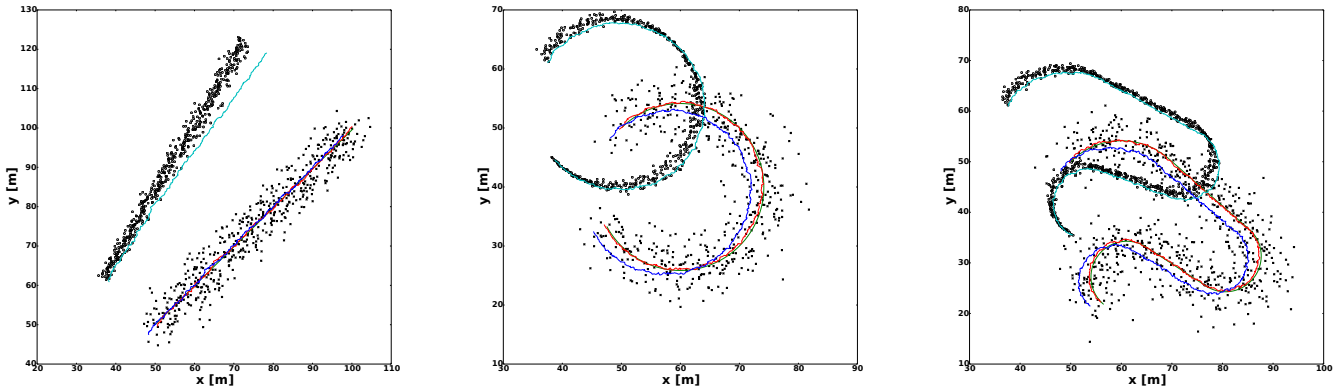

(a) Constant velocity model (b) Constant turn model (c) Complex model

Fig. 5: Performance of all approaches in high bias scenarios

TABLE I: Performance of the algorithm in low bias scenarios

Index	Given biases	Our estimated biases	Taylor-L.S. estimated biases	Our RMSE	Taylor-L.S. RMSE	Normal Meas. RMSE	Ideal Meas. RMSE
a	(0.1m, 0.05rad)	(0.195m, 0.049rad)	(0.225m, 0.051rad)	0.266m	0.255m	4.706m	0.209m
b	(0.1m, 0.05rad)	(0.188m, 0.051rad)	(0.177m, 0.053rad)	0.205m	0.248m	3.610m	0.196m
c	(0.1m, 0.05rad)	(0.195m, 0.048rad)	(0.168m, 0.050rad)	0.242m	0.227m	3.696m	0.219m

TABLE II: Performance of the algorithm in high bias scenarios

Index	Given biases	Our estimated biases	Taylor-L.S. estimated biases	Our RMSE	Taylor-L.S. RMSE	Normal Meas. RMSE	Ideal Meas. RMSE
a	(1.0m, 0.25rad)	(1.003m, 0.249rad)	(4.194m, 0.247rad)	0.281m	3.203m	23.670m	0.296m
b	(1.0m, 0.25rad)	(1.187m, 0.246rad)	(3.348m, 0.245rad)	0.415m	2.387m	17.895m	0.216m
c	(1.0m, 0.25rad)	(1.294m, 0.245rad)	(3.581m, 0.244rad)	0.531m	2.629m	18.846m	0.227m

[17] A. Drémeau, C. Schülke, Y. Xu, and D. Shah, "Statistical inference with probabilistic graphical models," *arXiv preprint arXiv:1409.4928*, 2014.
[18] F. Zhang and A. Knoll, "Systematic error modeling and bias estimation," *Sensors*, vol. 16, no. 5, p. 729, 2016.
[19] F. Dellaert, "Factor graphs and gtsam: A hands-on introduction," 2012.
[20] Y. Zhou, H. Leung, and M. Blanchette, "Sensor alignment with earth-centered earth-fixed (ecef) coordinate system," *Aerospace and Electronic Systems, IEEE Transactions on*, vol. 35, no. 2, pp. 410–418, 1999.